

**Photodissociation into $H(1S) + H(n=2)$ atoms:
Total and partial dissociation cross sections and relative importance
of dissociation and predissociation**

M. Glass-Maujean,* P. M. Guyon,[†] and J. Breton[‡]

Laboratoire pour l'Utilisation du Rayonnement Electromagnétique,

Centre National de la Recherche Scientifique et Université Paris—Sud, Bâtiment 209C, F-91405 Orsay Cedex, France

(Received 6 May 1985)

The total cross section for the photodissociation of H_2 into $H(1S) + H(n=2)$ between 85.0 and 77.0 nm has been measured using synchrotron radiation at high resolution (0.005-nm bandwidth). This continuum is made up of three contributions from B , $B' {}^1\Sigma_u^+$, and $C {}^1\Pi_u$. The B' photodissociation cross section is obtained directly at some excitation wavelengths from analysis of predissociation Fano profiles. The data are compared to computed values. The contribution of predissociated levels to the production of $H(n=2) + H(1S)$ atoms for white-light excitation is found to be more than two times more efficient than the direct photodissociation.

I. INTRODUCTION

First experimental evidence of the H_2 photodissociation continuum was obtained in 1926 by Dieke and Hopfield¹ and later Beutler² observed the various edges of this continuum associated with the various rotational levels of the ground state. Many years later Herzberg and Monfils³ reinvestigated this continuum near threshold and argued from the edge sharpness that the state responsible for the continuum could not present a potential hump, thus excluding the C state. The B -state continuum was expected to be insignificant because of small transition probabilities compared to those of both B' and C , just below the dissociation limit. These authors concluded that the continuum was essentially caused by $B' {}^1\Sigma_u^+$.⁴ Dalgarno and Allison (DA) calculated the B , C (Ref. 5), and B' (Ref. 6) photodissociation cross section and confirmed the dominant role of B' .

Measuring a photodissociation cross section by photoabsorption is usually difficult because of the likely occurrence of a high density of lines which may not be completely resolved and also of an ionization continuum which cannot be distinguished. Since the dissociation continuum leads to dissociation into $H(n=2) + H(1S)$, Mentall and Gentieu⁷ looked at the H Ly $_{\alpha}$ excitation spectrum at a low resolution (i.e., 0.1 nm). The data showed predissociated lines superimposed upon a continuum, the intensity of which was estimated with a large uncertainty to be consistent with the calculations.^{5,6}

In our previous work on the predissociation of hydrogen,⁸⁻¹⁰ we obtained high-resolution Ly $_{\alpha}$ excitation and absorption spectra in the 85.0–77.0-nm region. Most of the lines are well resolved which allowed us to investigate unambiguously the continuum and thus obtain a more precise determination of the photodissociation cross section.

Furthermore our previous study of the $D {}^1\Pi_u^+$ predissociated levels using Fano-profile analysis leads to the determination of the widths $\Gamma(v', J')$ and of the profile index q . In the present study we pursue this analysis further,

measuring the depths of the windows at the profile edges, and thus determine the $B' {}^1\Sigma_u^+$ interactive-continuum cross section which can thus be compared to the total $B + B' + C$ cross section.

Another problem of astrophysical interest connected with the dissociation into $H(n=2) + H(1S)$ is the relative importance of the dissociation versus predissociation in the $H(n=2)$ -atom formation. We compared the importance of the peaks of predissociated lines to the whole background in the Ly $_{\alpha}$ excitation spectrum.

II. EXPERIMENTAL

A. Experimental setup

The experimental arrangement has been described previously.⁸ Briefly, the vacuum-ultraviolet-radiation continuum from the Orsay electron storage ring was dispersed by a 3600-lines/mm platinum-coated holographic grating. A typical 0.005-nm bandwidth was achieved at 80 nm. The dispersed light crosses a differentially pumped, 30-cm-long cell maintained at a pressure of 10^{-2} Torr. Ly $_{\alpha}$ atomic fluorescence was detected through a $MgF_2 + O_2$ filter at right angles with the incident light beam, by an EMR 641 photomultiplier. An electric field is used to induce the $2 {}^2S-2 {}^2P$ transition.

The Ly $_{\alpha}$ excitation spectrum and the transmitted light were recorded simultaneously at a speed of 0.08 nm/min. The very low, dark current of the solar-blind Ly $_{\alpha}$ detector (i.e., 0.1 counts/sec) allowed the detection of a faint dissociation continuum. The number of Ly $_{\alpha}$ photons, counted between peaks, with a 0.03-nm bandwidth, varied from 80 to 4 with a dark current of about 2 counts. Near the cross-section maximum the bandwidth was narrowed to 0.01 nm.

B. Determination of the total absolute dissociation cross section for $B + C + B'$

The dissociation-continuum edges for $J''=0, 1, 2$, and 3 appear clearly in the Ly $_{\alpha}$ excitation spectrum, but only

one step associated with $J''=1$ is discerned in the absorption spectrum. Hence, the comparison of the $J''=1$ step heights in both spectra allows absolute calibration of the Ly α spectrum. The absorption cross section itself is determined using the Lambert law as discussed previously.¹⁰ The absorption spectrum of H₂ presents intense and broad Beutler-Fano profiles,^{11,12} which complicate the analysis of the continuum. The reported values of the photodissociation cross section are either measured far from these profiles or extrapolated through them. The reported error bars take into account the statistics and the pressure uncertainty.

C. $B'{}^1\Sigma_u^+$ photodissociation cross section and $B+C$ cross section

These perturbing Fano profiles can be used to determine the $B'{}^1\Sigma_u^+$ photodissociation cross section as they result from predissociation of $D^1\Pi_u^+(v',J')$ levels by the $B'{}^1\Sigma_u^+(J')$ continuum through Coriolis coupling with $\Delta J=0$. Near an isolated profile such as $R(J'')$, the absorption cross section can be written¹²

$$\sigma_{\text{abs}} = \sigma_B n_{J''} \mu_{J''} \frac{(q + \epsilon)^2}{1 + \epsilon^2} + \sigma_{\text{NI}}, \quad (1)$$

where $n_{J''}$ is the relative population of the J'' level, $\mu_{J''}$ the rotational line intensity of the $B'{}^1\Sigma_u^+ - X^1\Sigma_g^+$ transition, and σ_{NI} the cross section of all noninteractive continua (see the Appendix). The first term of Eq. (1) represents the Fano profile. For an incident photon energy such as $\epsilon = -q$, it goes to zero: it is the well-known window at the steep edge of the profile and for that particular wavelength the absorption cross section reduces to σ_{NI} . The noninteractive continua on the main profiles, the $R(0)$ and $R(1)$ lines, are the $B^1\Sigma_u^+$ and $C^1\Pi$ continua, together with the remaining B' ($J' \neq 1, 2$) continua; at room temperature, σ_{NI} is equal to

$$\sigma_{\text{NI}} = 0.31\sigma_B + \sigma_C + \sigma_B. \quad (2)$$

The details of such analysis are reported in the Appendix.

For each Fano profile we measured the noninteractive-continuum cross section and the window depth (i.e., the interactive-continuum cross section) after extrapolation of the total cross section. This gives us the determinations of σ_B , and $\sigma_B + \sigma_C$ for several points of the spectrum.

Another way to get the B' cross section is to use Eq. (23) from Fano's paper:¹²

$$\frac{1}{2}\pi(q^2 - 1)\Gamma = \frac{|\langle \varphi | T | i \rangle|^2}{|\langle \Psi_E | T | i \rangle|^2}, \quad (3)$$

where φ , Ψ_E , and i are the discrete, continuous, and fundamental states, respectively, T the optical transition operator, Γ the predissociation width of the profile, and q the profile index. This relation (3) occurs if q and Γ are fairly constant over the profile range.

Then, straightforwardly, the following relation can be obtained:

$$\sigma_{B'} = A_D(v') \frac{\lambda^2}{8\pi^2 c} \frac{1}{\Gamma_v(J''+1)} \frac{1}{q(J''+1)^2 - 1} \frac{J''+2}{J''+1} \quad (4)$$

for an $R(J'')$ line, $\sigma_{B'}$ being the B' cross section and

$A_D(v')$ the vibrational transition probability for the transition $D(v') - X(v''=0)$, both summed over all rotational lines. $\Gamma(J''+1)$, $q(J''+1)$, and $A_D(v')$ were measured previously^{9,10} [$A_D(v')$ was found to agree with theoretical predictions¹³].

This procedure leads to another determination of the B' cross section. The indicated error bars include the experimental uncertainties in Γ , q , and A but an ignored error remains in the validity of Eq. (3), that is, in the assumption of the constancy of q and Γ over the profile. This gives us a second determination of the $\sigma_{B'}$ cross section which can be compared to the previous one.

D. Relative importance of dissociation and predissociation

We compared the area of the background (due to the continuum) to the area of the peaks (due to predissociated discrete levels) in the Ly α excitation spectrum. The background was corrected for the dark current and incident-intensity drifts. A peak area represents the quantity $(I_0 - I_t)\Delta\lambda$ (I_0 is the incident light intensity, I_t the transmitted intensity, $\Delta\lambda$ the apparatus function), which is proportional to the absorption cross section integrated over the line profile only for an optically thin medium. The corrections described in Ref. 10 were applied systematically from 85.0 to 77.0 nm.

III. RESULTS AND DISCUSSION

A. Total photodissociation cross section

The different dissociation limits associated with the various rotational levels of the ground state were clearly observed. The amplitudes of the steps correspond to the rotational population at room temperature within experimental errors. Their positions and edge widths were found in agreement with previous photographic observations.³

The results are summarized in Fig. 1. The measured

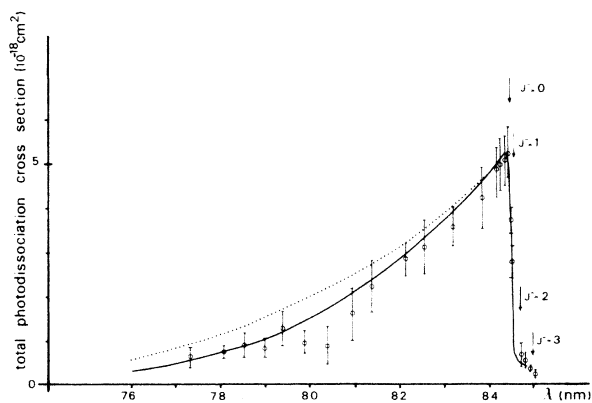


FIG. 1. Total cross section of photodissociation into H(1S) + H(n=2) in the 85–76-nm spectral range. Open circle, our measurements, with error bars; solid line, Glass-Maujean's calculations (Ref. 14); dotted line, calculations of Dalgarno and Allison (Ref. 6). The arrows indicate the various rotational edges of the continuum.

values are found to be in agreement with Glass-Maujean's computations¹⁴ on all the spectral range except two points. Despite the large error bars, DA's values are found to be systematically larger than the observed ones in the 81.0–77.0-nm range.

The observed values at 80.4 and 79.9 nm are below both calculations. This spectral range coincides with the opening of a new deexcitation channel ionization.

B. $B + C$ photodissociation cross section

The results are reported in Fig. 2. The two computations differ only slightly, the error bars involve both of them. The $B + C$ cross-section value at 80.4 nm shows the same behavior as the total cross section. One must notice that at 83.85 nm, the $B + C$ photodissociation represents around 25% of the total photodissociation which is hardly negligible.

This result corroborates our previous assertion¹⁵ and contradicts the commonly accepted overwhelming prevalence of the B' state in the photodissociation continuum. The C -state potential presents a maximum; therefore, its photodissociation can only be efficient at least 100 cm^{-1} above threshold.⁴ The nonobservation of a steep step in the photodissociation cross section for such values must only be caused by the slow increase of the C cross section above the potential hump.¹⁴

C. B' photodissociation cross section

The B' photodissociation cross-section values obtained through both determinations are reported in Fig. 3 with computed values. The situation is very similar to that observed for the total photodissociation, where the error bars cross Glass-Maujean's computed curve but are systematically below DA's values for wavelengths shorter than 82 nm. The discrepancy observed on the total cross section between DA's values and ours is due mainly to the B' -state contribution which confirms the discussion presented in the preceding paper.

Once again the value observed at 80.4 nm is below the computed curve: the B , C , and B' continua seem to

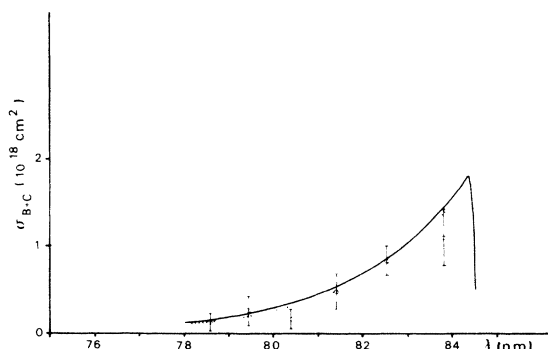


FIG. 2. Partial photodissociation cross section due to the $B' \Sigma_u + C' \Pi_u$ continua in the 85–78-nm spectral range; same as Fig. 1.

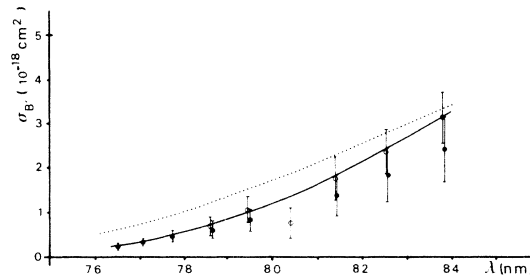


FIG. 3. Photodissociation cross section of the $B' \Sigma_u^+$ continuum. Open circles, measurements from the Fano-profile windows; solid circles, from Eq. (4); and same as Fig. 1.

present the same behavior when the ionization channel opens but we must remain careful about the validity of this assertion as these points are all dependent on the same single recording. Both determinations give compatible results: the values obtained through Eq. (4) are just slightly below those deduced from the profile windows. This constitutes a good test on the validity of Eq. (3) and provides experimental values in the 78.0–76.0-nm range.

D. Importance of dissociation and predissociation

The results are reported in Table I. They represent an integration of the spectrum from 85.0 to 77.0 nm. The precision is less than one might expect on such a long integration because the most intense peaks correspond to roughly 100% of the absorption, and the experimental error of these peaks is large.

The use of Figs. 2 and 3 gives us the relative importance of the B' and $B + C$ continua in the dissociation process. The most striking result is that direct dissociation leads to less than 30% of the whole $H(1S) + H(n=2)$ formation and the B' continuum to less than 25%. If the B' dissociation is found to be less efficient, as believed, it is indirectly the major contribution, as all the predissociation observed yielding $H(1S) + H(n=2)$ atoms are due to couplings with the B' state.^{16,8} Then from dissociation or predissociation, the B' state is responsible for more than 90% of the $H(1S) + H(n=2)$ formation between 85 and 77 nm. That means that the ratio of the number of atoms of $H(2S)$ to the number of $H(2P)$ atoms is mainly determined by the B' behavior at large internuclear distance¹⁷ as well as the angular distribution of the scattered atoms and the polarization of the Ly_α $2P-1S$ emitted light.¹⁸

E. Comparison with electron-impact data

If the photodissociation process in H_2 has been only scarcely studied, electron-impact dissociation in H_2 has been intensively investigated, both theoretically¹⁹ and experimentally.^{20–24} We have seen that photodissociation products $H(1S) + H(n=2)$ were mainly determined by the B' state, which is known to yield a mixing of $H(2S)$ and $H(2P)$.¹⁷ Depending on the authors, the $H(2S)$ yield

TABLE I. Various photodissociation process yields over the 85–76-nm spectral range: importance of the various continua and predissociations in the H(1S) + H(n=2) production (first column), H(2²P) and H(2²S) (second and third columns) assuming Borondo's ratio (Ref. 17); importance of the various processes in the H(2²S) formation (fourth column), to be compared to the results of Lamb *et al.* (Ref. 24) in the last column.

	$\sigma_i(n=2)/\sum\sigma_i(n=2)$	$\sigma_i(2^2P)/\sum\sigma_i(n=2)$	$\sigma_i(2^2S)/\sum\sigma_i(n=2)$	$\sigma_i(2^2S)/\sum\sigma_i(2^2S)$	Lamb <i>et al.</i>
<i>B'</i> continuum	23%	7%	16%	24%	
<i>C</i> continuum	} 7%	} 30%	} 13%	} 17%	}
<i>B</i> continuum					
<i>D</i> predissociation	21%	6%	15%	22%	} 49%
<i>B''</i> predissociation	25%	8%	17%	27%	
Other predissociations	24%	7%	17%	26%	

varies from 70% to 57% remaining very far from the electron-impact measured ratio²⁰ of 33% for incident energies located between 50 and 500 eV. We conclude therefore that electron-impact dissociation must involve a significant contribution from non-optically-allowed levels which must contribute more to the H(2P)-atom formation than to the H(2S) formation.

The dissociation and predissociation processes discussed here are located in the 0–1.5-eV range above threshold: they can only be compared to the “slow” atom-formation processes²¹ in the electron-impact experiments.

For the H(2S) slow atom formation, optically allowed levels were found to be dominant in the process^{22–24} and Wing *et al.*²⁴ estimated the predissociation's importance at 42%. They were able to resolve only *D* and *B''* structures. If we isolate these series in our spectrum, our data agree quite well with theirs, confirming previous conclusions on the major contribution of optically allowed levels in the H(2S) slow atom formation (see Table I).

Our data clearly disagree with the assertion of Chung Liu and Lee. Their calculated *B'* dissociation cross section by electron impact found in fair agreement with the H(2S) formation cross section led them to conclude to the major *B'* contribution in the process. They neglected the “fast” H(2S) atoms production which cannot proceed from the *B'* state and they ignored that the *B'* continuum does not produce H(2S) atoms only. Therefore, their main argument fails.

IV. CONCLUSION

The total photodissociation cross section yielding H(1S) + H(n=2) atoms in the 84.5–77.5-nm spectral range had been measured and found in agreement with

$$\begin{aligned}
 & n_{J'+1} |\langle \Psi_E(J') | \mathbf{e} \cdot \mathbf{r} | X, J'' = J+1 \rangle|^2 + n_{J'-1} |\langle \Psi_E(J') | \mathbf{e} \cdot \mathbf{r} | X, J'' = J-1 \rangle|^2 \\
 & = n_{J'+1} |\langle \underline{\psi}_E(J') | \mathbf{e} \cdot \mathbf{r} | X, J' = J+1 \rangle|^2 (q_{J'+1}^{J'} + \epsilon_{J'+1}^{J'})^2 / [1 + (\epsilon_{J'+1}^{J'})^2] \\
 & + n_{J'-1} |\langle \underline{\psi}_E(J') | \mathbf{e} \cdot \mathbf{r} | X, J'' = J-1 \rangle|^2 (q_{J'-1}^{J'} + \epsilon_{J'-1}^{J'})^2 / [1 + (\epsilon_{J'-1}^{J'})^2],
 \end{aligned}
 \tag{A2}$$

ab initio adiabatic calculations. Taking advantage of the strong predissociated lines, we were able to investigate the relative importance of *B'* and *B* + *C* in the continua; the *B* + *C* contribution is clearly smaller than the *B'* one but not negligible as believed before.

Predissociation is found much more efficient than direct dissociation. Such results may make some astrophysical evaluations doubtful.

APPENDIX

The predissociated levels $D^1\Pi_u^+(v', J')$ are coupled to $B'^1\Sigma_u^+(E, J')$. The v' levels are far from their neighbors ($v' \pm 1$) and can be isolated; the J' continua are related one to one to the J' discrete levels, and constitute J' independent systems, yielding to a mere superposition in the total signal.

For each J' pair of levels, the eigenvector is of the form [Ref. 12, Eq. (16) (keeping Fano's notation)]

$$\Psi_E(J') = \frac{1}{\pi V_E^*(J')} \sin[\Delta(J')] \Phi(J') - \cos[\Delta(J')] \psi_E(J').
 \tag{A1}$$

$\Phi(J)$ is the modified discrete state.

Photoabsorption to this state from the ground state can occur through two transitions, $R(J'-1)$ and $P(J'+1)$. The two rotational levels $J'' = J' \pm 1$ are incoherently populated with a Boltzmann distribution. Let $n_{J''}$ be the relative population of the J'' level (i.e., $\sum_{J''} n_{J''} = 1$), the photoabsorption probability for a J' couple is proportional to

$\epsilon_{J'+1}^{J'}$ and $\epsilon_{J'-1}^{J'}$ are null for the same energy but not for the same excitation wavelength. $\Psi_E(J')$ is the unperturbed continuum state. Let $\mu_{J''}^{J'}$ be the rotational line intensity of the $B' \rightarrow \Sigma_u^+$ transition such that $\sum_{J''} \mu_{J''}^{J'} = 1$; then the total photoabsorption cross section for the predissociated state P and interactive continua I is

$$\sigma_{P,I} = \sigma_{B'} \left[\sum_{J'} n_{J'+1} \mu_{J'+1}^{J'} (q_{J'+1}^{J'} + \epsilon_{J'+1}^{J'})^2 / [1 + (\epsilon_{J'+1}^{J'})^2] + n_{J'-1} \mu_{J'-1}^{J'} (q_{J'-1}^{J'} + \epsilon_{J'-1}^{J'})^2 / [1 + (\epsilon_{J'-1}^{J'})^2] \right] \quad (\text{A3})$$

neglecting the smooth variations of $\sigma_{B'}$ on the J' energy progression.¹⁴ The noninteractive continua are B and C and the remaining $J'=0$ of the B' state corresponding to the $P(1) B'-X$ transition.

The total absorption cross section is then equal to

$$\sigma = \sigma_{P,I} + n_{J'=1} \mu_1^0 \sigma_{B'} + \sigma_C + \sigma_B. \quad (\text{A4})$$

The various parameters of Eqs. (A3) and (A4) are easily determined:⁸

$$q_{J'-1}^{J'} = q_{J'-2}^{J'-1} (J'-1) / J' \quad (\text{A5})$$

with $q_0^1 = 18$,

$$q_{J'+1}^{J'} = q_{J'-1}^{J'} J' / (J'+1), \quad (\text{A6})$$

$$\mu_{J'-1}^{J'} = J' / (2J'-1), \quad \mu_{J'+1}^{J'} = (J'+1) / (2J'+3),$$

and

$$\epsilon_{J'\pm 1}^{J'} = (\bar{\sigma} - \bar{\sigma}_{J'\pm 1}^{J'}) / \frac{1}{2} \Gamma(J'), \quad (\text{A7})$$

where $\bar{\sigma} = 1/\lambda$, $\bar{\sigma}_{J'\pm 1}^{J'} = 1/\lambda_{J'\pm 1}^{J'}$. $\lambda_{J'\pm 1}^{J'}$ is the wavelength excitation of the perturbed discrete level through a $P(J'+1)$ line and an $R(J'-1)$ line, respectively,

$$\Gamma(J') = \Gamma(J'=1) J'(J'+1) / 2, \quad (\text{A8})$$

due to rotational coupling. $\Gamma(J'=1)$ are from Ref. 8.

At 83.85 nm, the main contributions of $\sigma_{P,I}$, those from $R(1)$ and $R(0)$ (within 0.005 nm), go to zero and

$$\epsilon_1^2 = -q_1^2 \quad \text{and} \quad \epsilon_0^1 = -q_1^2. \quad (\text{A9})$$

This situation corresponds to what we called in Sec. III the "windows at the steep edge of the profiles." The other profiles located at longer wavelengths are partly contributing: one can evaluate, at room temperature,

$$\sigma_{P,I}(83.85 \text{ nm}) = 0.09 \sigma_{B'}. \quad (\text{A10})$$

Then

$$\sigma = 0.31 \sigma_{B'} + \sigma_C + \sigma_B. \quad (\text{A11})$$

Such a situation occurs for the whole vibrational progression, the numerical value of Eq. (A11) remaining roughly unchanged.

*Also at Laboratoire de Spectroscopie Hertzienne de l'Ecole Normale Supérieure, Université Pierre et Marie Curie, 4 place Jussieu, F-75230 Paris Cedex 05, France.

†Also at Laboratoire des Collisions Atomiques et Moléculaires, Université Paris—Sud, Bâtiment 351, F-91405 Orsay Cedex, France.

‡Also at Laboratoire d'Electrodynamique des Gaz Ionisés, Université Pierre et Marie Curie, 4 place Jussieu, F-75230 Paris Cedex 05, France.

¹G. H. Dieke and J. J. Hopfield, *Z. Phys.* **40**, 299 (1926); *Phys. Rev.* **30**, 400 (1927).

²H. Beutler, *Z. Phys. Chem. B* **29**, 315 (1935).

³G. Herzberg and A. Monfils, *J. Mol. Spectrosc.* **5**, 482 (1960).

⁴I. Dabrowski and G. Herzberg, *Can. J. Phys.* **52**, 1110 (1974).

⁵A. C. Allison and A. Dalgarno, *At. Data* **1**, 91 (1969).

⁶A. Dalgarno and A. C. Allison, *J. Geophys. Res.* **74**, 4178 (1969).

⁷J. E. Mentall and E. P. Gentieu, *J. Chem. Phys.* **52**, 5641 (1970).

⁸M. Glass-Maujean, J. Breton, and P. M. Guyon, *Chem. Phys. Lett.* **63**, 591 (1979).

⁹P. M. Guyon, J. Breton, and M. Glass-Maujean, *Chem. Phys. Lett.* **68**, 314 (1979).

¹⁰M. Glass-Maujean, J. Breton, and P. M. Guyon, *Chem. Phys. Lett.* **112**, 25 (1984).

¹¹H. Beutler, A. Deubner, and H. O. Jünger, *Z. Phys.* **98**, 181

(1935).

¹²U. Fano, *Phys. Rev.* **124**, 1866 (1961).

¹³M. Glass-Maujean, *At. Data Tables* **30**, 301 (1984).

¹⁴M. Glass-Maujean, preceding paper, *Phys. Rev. A* **33**, 342 (1986).

¹⁵M. Glass-Maujean, J. Breton, and P. M. Guyon, *J. Chem. Phys.* **83**, 1468 (1985).

¹⁶A. Monfils, *Bull. Acad. R. Belg. Cl. Sci.* **47**, 816 (1961).

¹⁷J. E. Mentall and P. M. Guyon, *J. Chem. Phys.* **67**, 3845 (1977); I. V. Komarov and V. N. Ostrovsky, *Pis'ma Zh. Eksp. Teor. Fiz.* **28**, 446 (1978) [*JETP Lett.* **28**, 413 (1978)]; F. Borondo, L. R. Eguiaray, and A. Riera, *J. Phys. B* **15**, 899 (1982).

¹⁸S. J. Singer, K. F. Freed, and Y. B. Band, *J. Chem. Phys.* **79**, 6060 (1983).

¹⁹S. Chung, C. C. Lin, and E. T. P. Lee, *Phys. Rev. A* **12**, 1340 (1975).

²⁰D. A. Vroom and F. J. de Heer, *J. Chem. Phys.* **50**, 580 (1969).

²¹M. Leventhal, R. T. Robiscoe, and K. R. Lea, *Phys. Rev.* **158**, 49 (1967).

²²J. W. Czarnik and C. E. Fairchild, *Phys. Rev. Lett.* **26**, 807 (1971).

²³M. Misakian and J. C. Zorn, *Phys. Rev. A* **6**, 2180 (1972).

²⁴S. R. Ryan, J. J. Spezeski, O. F. Kalman, W. E. Lamb, Jr., L. C. McIntyre, Jr., and W. H. Wing, *Phys. Rev. A* **19**, 2192 (1979).